Supplementary materials

Materials and Methods

Imbibition strength of blotter

The imbibition strength of the blotter used in the experiment is characterized from capillary rise experiment. A strip of length 25cm, width 2cm and thickness 1mm is brought in to contact with a container filled with water (see Fig.S1A). Images are taken every 15s with a digital camera. We measured the position of the imbibition front as a function of time and plot the data in a log-log scale (see Fig.S1B). The imbibition rises up the strip as the square root of time. Using a fitting function of the form $\sqrt{2Dt}$, where the diffusive coefficient D is the only free parameter, we obtain $D = 2.6 \times 10^{-6}\text{m}^2/\text{s}$. When using a fitting function of the form $(2D)^n$ where D and n are free parameters, we obtain n=0.45 and $D = 4.9 \times 10^{-6}\text{m}^2/\text{s}$. The dynamics of the imbibition front is therefore nearly diffusive with a diffusive coefficient $D \sim 4 \times 10^{-6}\text{m}^2/\text{s}$.

Solid volume fraction of the suspension

We measure the solid volume fraction of suspension when coming out of the nozzle varying the flux Q and for three nozzle diameters $d_1 = 1.19$mm, $d_2 = 1.6$mm and $d_3 = 2.0$mm. To measure the solid volume fraction Φ_s, the suspension is poured in a small container at a fixed Q and we measure the weight m_{sus} of the content using a precision scale. The container is then placed on a hot plate for several hours until the liquid completely evaporates and we measure the weight m_{sol} of the content which is now made of dry, non-cohesive grains. The weight of the liquid is $m_{liq} = m_{sus} - m_{sol}$. Using the density of the liquid (water) ρ_{liq}=0.9 and the grains $\rho_{sol} = 1.4$, we can extract the solid volume fraction $\Phi_s = (m_{sol}/\rho_{sol})/(m_{sol}/\rho_{sol} + m_{liq}/\rho_{liq})$. Φ_s is found to be lower than the solid volume fraction of the sedimented grains inside the syringe (~0.6), and increases with the flux as shown in Fig.2A. No dependence with the nozzle diameter is observed. For $\Phi_s \sim 0.55$, the effective viscosity can be estimated to be $\mu_{eff} \sim 500$mPa.s *(16)*

Jet breakup length

We characterize the transition from dripping to jetting by measuring the breakup length L_{RP} varying the flux (Fig.1C) and without the substrate (*i.e.* $H = \infty$). For low flux ($Q < 2$mL/s), the jet breaks into droplets at a fixed distance from the nozzle leading to a dripping with a well-defined frequency. As the flow speed increases, the point of breakup moves rapidly away from the nozzle, leading to the formation of a jet. The breakup length L_{RP} of the jet is found to increase linearly with the flux Q ($Q > 2$mL/s).

In principle, the dependence of the breakup length with the flux Q can be explained using the Rayleigh-Plateau instability of a liquid cylinder of radius r. The growth rate of the most unstable mode in the inertial regime is $\sigma \sim \sqrt{\gamma/(r^3\rho)}$, where ρ is the density and is $\sigma \sim \gamma/(\mu r)$ in the viscous regime where μ is the viscosity. Following *(S1),* we derive the breakup length, we have $L_{RP} = \alpha\pi^{6/7}/2(\rho/\gamma)^{4/7}g^{1/7}Q^{6/7}$ (low viscosity limit) where α is close to unity and $L_{RP} = A\,Q^{2/3}$ (high viscosity limit) where the dimensional prefactor is given in *(S1)*. The 2/3 law is in the correct range of length while the linear trend is not captured whereas the 6/7 law is closer to the linear trend but $\alpha = 200 \gg 1$. Thus, none of these laws give a satisfying explanation for the linear trend observed and further investigations need to be performed to clarify this aspect.
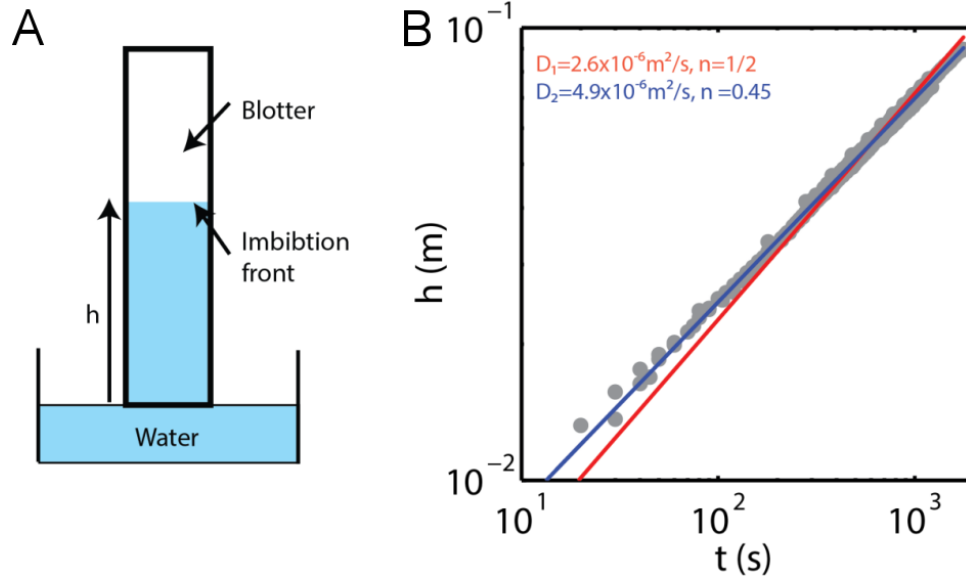
Figure S1 : (A) Schematics of the capillary rise setup where a strip of blotter paper is dipped in a container filled with water. At $t = 0$s, the blotter is in contact with the water and the position h of the imbibition front separating the wet and the dry section is measured over time. **(B)** Log-log plot of h as function of time t. Using a fitting function of the form $\sqrt{2Dt}$ (red line), we obtain $D = 2.6 \times 10^{-6} \text{m}^2$/s. Using a fitting function of the form $(2D)^n$, we obtained $n = 0.45$ and $D = 4.9 \times 10^{-6} \text{m}^2$/s.

Movie captions

Movie S1: Movie of granular suspension deposited on a translating substrate. Arches are observed to form when the substrate switched from an impermeable plastic to a dry granular bed composed of the same glass beads as used in the suspension which acts as a superabsorder for the liquid in the suspension. Flow rate $Q = 0.18$ mL/s, substrate speed $V_s= 1.4$cm/s, nozzle height $H=10$mm, and nozzle diameter $d = 2$mm. Image acquisition rate is 40 frames/s and playback 20 frames/s. The suspension spreads like a viscous liquid when it comes in contact with the solid plastic substrate. However, spontaneous formation of arches is observed when the liquid is quickly absorbed by the porous substrate because of capilary action.

Movie S2: Movie of granular suspension deposited on a thin blotter paper which is translated horizontally. Flow rate $Q = 0.22$mL/s, substrate speed $V_s=24$cm/s, nozzle height $H = 19$mm, and nozzle diameter $d = 2.0$mm. Image acquisition rate 500 frames/s and playback 10 frames/s. Upon impact, the jet is observed to exhibit limited spreading on the substrate before complete solidification occurs leaving a continuous horizontal thread.

Movie S3: Movie of granular suspension dripped on a thin blotter paper which is slightly tilted by an angle of 2 degrees with respect to the horizontal to change the drop height H, linearly. Flow rate $Q = 0.044$mL/s, substrate speed $V_s = 2.4$cm/s, nozzle height $H = 15.6 – 5.4$mm, and nozzle diameter $d = 1.194$mm. Image acquisition rate 333 frames/s and playback 10 frames/s. Upon impact, the drop is observed to exhibit limited spreading on the substrate before complete solidification occurs. Oblate shapes and almost spherical shapes are obtained at high and low impact speed, respectively.

Movie S4: Movie of granular suspension deposited on a thick blotter paper which is translated horizontally. Flow rate $Q = 0.088$mL/s, substrate speed $V_s=4.8$cm/s, nozzle height $H = 2.3$mm and nozzle diameter d = 2mm. Image acquisition rate 333 frames/s and playback 10 frames/s. The spreading of the suspension occurs at the same timescale as the pinchoff leaving behind a solid structure in the shape of a hook.

Movie S5: Movie of granular suspension deposited on a thin blotter slightly tilted and translated horizontally. Flow rate $Q = 0.18$mL/s, substrate speed $V_s=2.4$cm/s, nozzle height $H = 13.5$ mm, and nozzle diameter $d = 1.19$mm. Image acquisition rate 333 frames/s and playback 10 frames/s. Upon impact, the jet solidifies in the shapes of an undulating, periodic structure characterized by an arch with a small span length followed by a longer one.

Movie S6: Movie of granular suspension deposited on a thick blotter translated horizontally. Flow rate $Q =1.7$mL/s, substrate speed $V_s= 1.2$cm/s, nozzle height $H = 25.4$mm, and nozzle diameter $d = 2$mm. Image acquisition rate 50 frames/s and playback 10 frames/s. At large flow rate, formation of ripples is still observed at the bottom but a secondary instability leads to larger meanders.

REFERENCES CITED IN MATERIALS AND METHODS

S1 : A. Javadi, J. Eggers, D. Bonn, M. Habibi, N. Ribe *Phys. Rev. Lett.* **110**, 144501 (2013).